Supporting Information for

Effects of the dynamic effective porosity on watertable fluctuations and seawater intrusion in coastal unconfined aquifers

Zhaoyang Luo[1,2,#], Jun Kong[1,3,#], Lili Yao[4], Chunhui Lu[1], Ling Li[5,6], David Andrew Barry[2]

[1]State Key Laboratory of Hydrology-Water Resources and Hydraulic Engineering, Hohai University, Nanjing, China
[2]Ecological Engineering Laboratory (ECOL), Environmental Engineering Institute (IIE), Faculty of Architecture, Civil and Environmental Engineering (ENAC), École Polytechnique Fédérale de Lausanne (EPFL), Lausanne, Switzerland
[3]Key Laboratory of Coastal Disaster and Protection (Ministry of Education), Hohai University, Nanjing, China
[4]Department of Civil, Environmental, and Construction Engineering, University of Central Florida, Orlando, USA
[5]School of Engineering, Westlake University, Hangzhou, China
[6]School of Civil Engineering, The University of Queensland, Brisbane, Australia

[#]Corresponding authors: Zhaoyang Luo (zhaoyang.luo@epfl.ch) and Jun Kong (kongjun999@126.com)

Contents of this file

Figures S1-S5

Introduction

Figure S1 shows a schematic diagram of an unconfined aquifer.

Figure S2 shows the experimental apparatus used to quantify the dynamic effective porosity.

Figure S3 plots amplitude decay rate (k_rD) and phase lag increase rate (k_iD) versus non-dimensional aquifer depth ($n_e\omega D/K_s$) for watertable waves obtained from experiments and different existing theories.

Figure S4 plots amplitude decay rate (k_rD) and phase lag increase rate (k_iD) versus non-dimensional aquifer depth ($n_e\omega D/K_s$) for watertable waves obtained from experiments and existing theory that combines equation (2) with the complex-valued expression for the dynamic effective porosity proposed by Cartwright et al. (2005).

Figure S5 gives the numerical model setup for the base case.

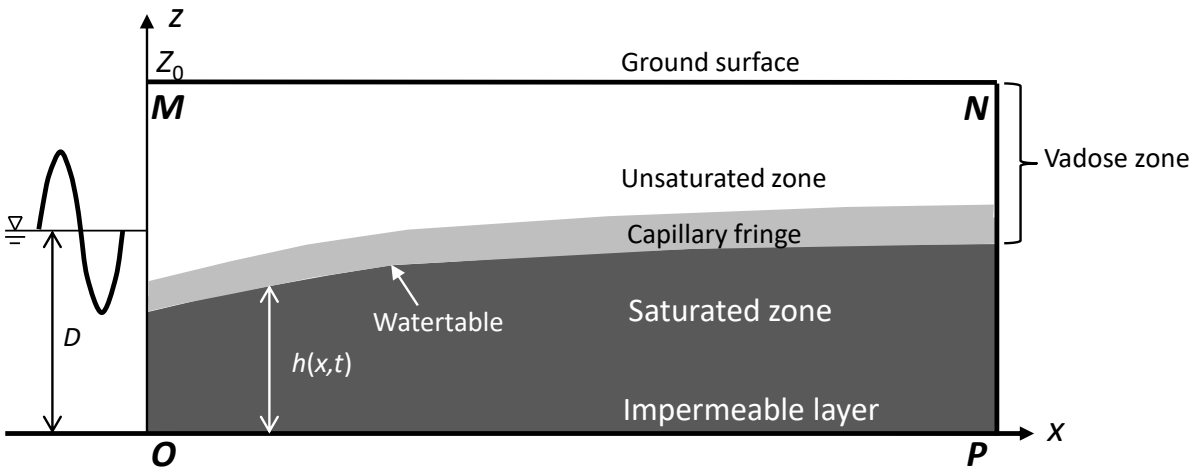

Figure S1. Schematic diagram of an unconfined aquifer (modified from Kong et al. (2015)). *OPNM* represents the aquifer normal to the shoreline with a vertical sea boundary (*OM*). *OP* and *PN* are impermeable while *MN* is the ground surface, *t* [T] is time, *x* [L] is the horizontal distance from the vertical seaward boundary, *D* [L] is the aquifer depth (equal to the mean height of the boundary forcing), and *h* [L] is the watertable height above the impermeable layer.

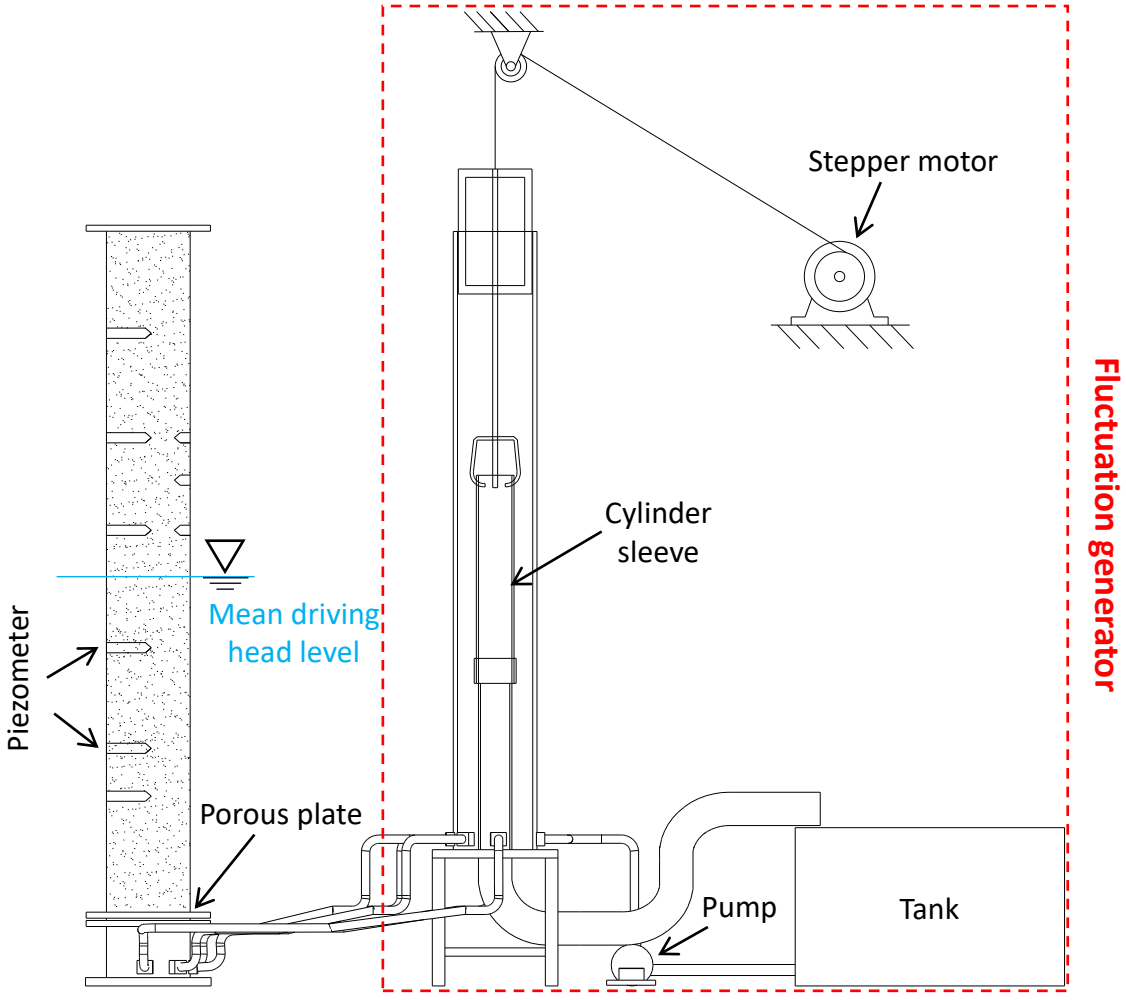

Figure S2. Experimental apparatus used to quantify the dynamic effective porosity, modified from Luo et al. (2020).

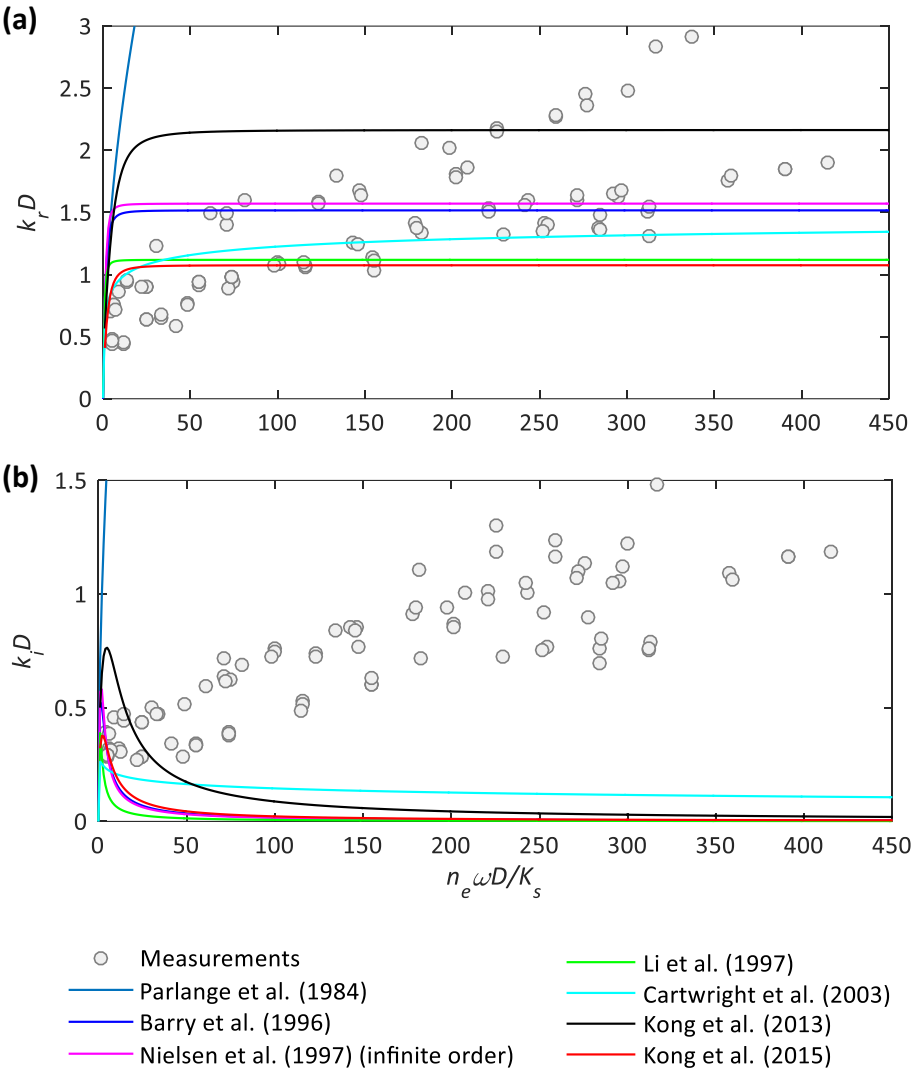

Figure S3. Comparison of (a) amplitude decay rate (k_rD) versus non-dimensional aquifer depth ($n_e\omega D/K_s$) and (b) phase lag increase rate (k_iD) versus non-dimensional aquifer depth ($n_e\omega D/K_s$) for watertable waves obtained from experiments and different existing theories. Parameters used are consistent with Shoushtari et al. (2016): D = 0.92 m, H_ψ = 0.61 m and K_s = 4.7×10^{-4} m/s. Parameter definitions are given in the main text.

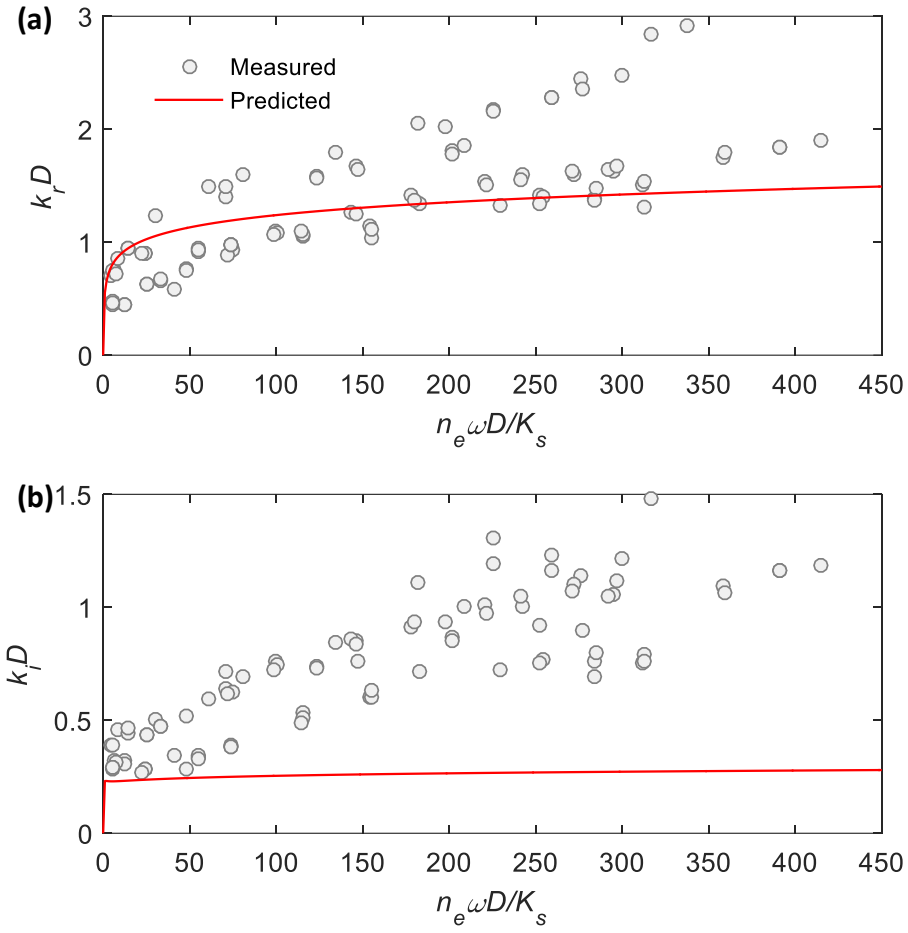

Figure S4. Comparison of (a) amplitude decay rate (k_rD) versus non-dimensional aquifer depth ($n_e\omega D/K_s$) and (b) phase lag increase rate (k_iD) versus non-dimensional aquifer depth ($n_e\omega D/K_s$) for watertable waves obtained from experiments and existing theory that combines equation (2) with the complex-valued expression for the dynamic effective porosity proposed by Cartwright et al. (2005). Parameters used are consistent with Shoushtari et al. (2016): D = 0.92 m, H_ψ = 0.61 m and $K_s = 4.7 \times 10^{-4}$ m/s.

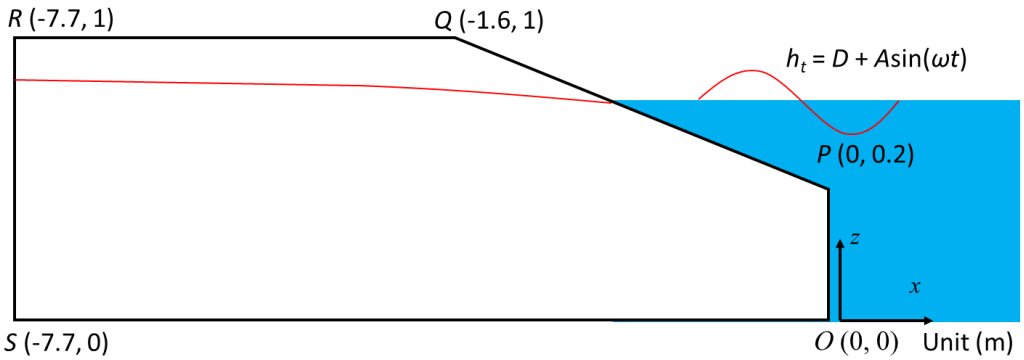

Model setup

Boundary conditions:

RS: Constant head boundary with h = 0.74 m and c = 0 ppt

OPQ: Time-dependent head boundary with D = 0.7 m, A = 0.075 m and T = 240 s ($\omega = 2\pi/T$), and c = 35 ppt

OS: No flow boundary

QR: Atmospheric boundary

Initial conditions:

h = 0.70 m, c = 0 ppt

Soil properties:

VG parameters: α = 11 m^{-1}, n = 6,

Hydraulic conductivity: $K_s = 3 \times 10^{-3}$ m/s

Static effective porosity: 0.4

Diffusion coefficient: 1×10^{-9} m^2/s

Longitudinal dispersivity: 0.006 m

Transversal dispersivity: 0.0006 m

Mesh sizes and time step:

Δx = 0.02 m, Δz = 0.1 m and Δt = 4 s

Figure S5. Numerical model setup for the base case (Shen et al., 2020), which uses a van Genuchten (VG) soil.

References

Barry, D. A., Barry, S. J., & Parlange, J.-Y. 1996. Capillarity correction to periodic solutions of the shallow flow approximation, In *Mixing Processes in Estuaries and Coastal Seas, C. B. Pattiaratchi (editor), Coastal and Estuarine Studies*, Volume 50, American Geophysical Union, Washington, DC, pp. 496–510. https://doi.org/10.1029/CE050

Cartwright, N., Nielsen, P., & Dunn, S. (2003). Water table waves in an unconfined aquifer: Experiments and modeling. *Water Resources Research*, *39*(12), 1330. https://doi.org/10.1029/2003WR002185

Li, L., Barry, D. A., Parlange, J.-Y., & Pattiaratchi, C. B. (1997). Beach water table fluctuations due to wave run-up: Capillarity effects. *Water Resources Research*, *33*(5), 935-945. https://doi.org/10.1029/96WR03946

Luo, Z., Kong, J., Ji, Z., Shen, C., Lu, C., Xin, P., Zhao, Z., Li, L., & Barry, D. A. (2020). Watertable fluctuation-induced variability in the water retention curve: Sand column experiments. *Journal of Hydrology*, *589*, 125125. https://doi.org/10.1016/j.jhydrol.2020.125125

Nielsen, P., Aseervatham, R., Fenton, J. D., & Perrochet, P. (1997). Groundwater waves in aquifers of intermediate depths. *Advances in Water Resources*, *20*(1), 37–43. https://doi.org/10.1016/S0309-1708(96)00015-2

Kong, J., Shen, C.-J., Xin, P., Song, Z., Li, L., Barry, D. A., Jeng, D.-S., Stagnitti, F., Lockington, D. A., & Parlange, J.-Y. (2013). Capillary effect on water table fluctuations in unconfined aquifers. *Water Resources Research, 49*(5), 3064–3069. https://doi.org/10.1002/wrcr.20237

Kong, J., Xin, P., Hua, G.-F., Luo, Z.-Y., Shen, C.-J., Chen, D., & Li, L. (2015). Effects of vadose zone on groundwater table fluctuations in unconfined aquifers. *Journal of Hydrology, 528*, 397–407. https://doi.org/10.1016/j.jhydrol.2015.06.045

Parlange, J.-Y., Stagnitti, F., Starr, J. L., & Braddock, R. D. (1984). Free-surface flow in porous media and periodic solution of the shallow-flow approximation. *Journal of Hydrology*, *70*(1-4), 251-263. https://doi.org/10.1016/0022-1694(84)90125-2

Shen, Y., Xin, P., & Yu, X. (2020). Combined effect of cutoff wall and tides on groundwater flow and salinity distribution in coastal unconfined aquifers. *Journal of Hydrology*, *581*, 124444. https://doi.org/10.1016/j.jhydrol.2019.124444